An X-ray Absorption Fine Structure Study of the Sulfidation Behavior of CoNaY Prepared by Ion Exchange: The Influence of Physisorbed Water and Cobalt Loading

Petra W. de Bont,[†] Marcel J. Vissenberg,[‡] V. H. J. (San) de Beer,[‡] J. A. Rob van Veen,[‡] Rutger A. van Santen,[‡] and Adri M. van der Kraan*,[†]

Interfacultair Reactor Instituut, Delft University of Technology, Mekelweg 15, 2629 JB Delft, The Netherlands, and Schuit Institute of Catalysis, Eindhoven University of Technology, P.O. Box 513, 5600 MB, Eindhoven, The Netherlands

Received: March 6, 1998

The influence of physisorbed water on the sulfidation of a 4 wt % cobalt containing ion exchanged CoNaY catalyst is studied by X-ray absorption near edge structure (XANES) and extended X-ray absorption fine structure (EXAFS) and high resolution electron microscopy (HREM). Upon dehydrating ion exchanged CoNaY, the Co^{2+} ions migrate into the zeolite cation positions. This migration has a large influence on the catalyst sulfidation behavior. In the presence of physisorbed water sulfidation results in the formation of large Co_9S_8 particles at the outer surface of the zeolite. On the contrary, formation of highly dispersed "Co−sulfide" species inside the zeolite cavities is observed when the physisorbed water is removed prior to sulfidation. The above findings confirm those obtained by Mössbauer emission spectroscopy (MES) and thiophene HDS activity measurements reported earlier (de Bont, P. W.; Vissenberg, M. J.; Boellaard, E.; van Santen, R. A.; de Beer, V. H. J.; van der Kraan, A. M. *Bull. Soc. Chim. Belg.* **1995**, *104*, 205). The dispersion of the Co−sulfide species formed after sulfidation at 673 K is not affected by varying the amount of cobalt (2, 4, and 8 wt %) in the dehydrated NaY zeolite as shown by the EXAFS and MES experiments.

Introduction

The hydrocracking process is designed to produce high yields of middle distillate products and often consists of two separate stages. The first stage is a hydrotreatment step using a sulfur resistant catalyst for the removal of heteroatoms such as, for instance, sulfur (HDS) and nitrogen (HDN) and the mild hydrogenation of aromatic structures. In the second stage the actual hydrocracking occurs, using a catalyst which combines hydrogenation (metal sites) and cracking (acidic sites) functions. Small transition metal−sulfide particles in acidic zeolites provide the possibility to combine these two functions in one catalytic system, such as in the case of NiW/ASA.[2]

As the catalytic activity will depend on the dispersion of the active phase, an attendant advantage of using zeolites is that they have a well defined pore system which creates the possibility to prepare catalysts containing very small uniformly shaped metal−sulfide particles inside the zeolite cavities. For this reason, these catalyst systems are not only interesting for their potential application in hydrocracking processes but also for checking the relevance of a "structural model" for "Co−sulfide" species present in conventional Co−Mo−sulfide based hydrotreating catalysts as proposed by Crajé et al.[3−7] This model predicts among other things a relation between particle size and/or ordering of these Co−sulfide species and a parameter viz. the quadrupole splitting (QS) measured by means of Mössbauer emission spectroscopy (MES).

In spite of the fact that stabilized Y (USY) zeolites are most commonly used for industrial hydrocracking,[8,9] the original NaY is used as support for our model catalysts to avoid changes in catalytic properties, dispersion or degree of sulfidation of the metal−sulfide phase caused by the extra framework alumina and the mesopores present in the stabilized Y zeolite.[10]

The formation of cobalt−sulfide particles inside NaY has already been studied by MES[1,11] It is found that upon sulfidation in presence of physisorbed water in ion exchanged CoNaY (referred to as wet CoNaY)[1] and in an impregnation type Co/NaY,[11] Co−sulfide particles are formed with a low QS value (0.22 mm/s), comparable with the QS value obtained for Co_9S_8[12], and that these particles had a relatively low HDS activity. However, when in the case of ion exchanged CoNaY the physisorbed water is removed prior to sulfidation (referred to as dry CoNaY), Co−sulfide species with a rather high QS value (0.63 mm/s) and a relatively high initial thiophene HDS activity were formed.[1]

The present study deals with the EXAFS results obtained for sulfided wet and dry ion exchanged CoNaY. Only a few preliminary qualitative EXAFS results have been presented earlier.[1] Besides, the influence of the cobalt loading on the dispersion of the Co−sulfide particles is studied by EXAFS as well as MES.

Experimental Section

Catalyst Preparation and Treatment. For this EXAFS study Co(x)NaY catalysts (x = 2.4, 4.0, or 8.5 wt % Co, calculated on the basis of the waterfree NaY) were prepared by ion exchange of 10 g NaY (ZI, $Na_{53}(AlO_2)_{53}(SiO_2)_{139}$, containing 24 wt % physisorbed water) with 250 mL of 0.012 M, 0.02 M, or 1 M solutions of $CoCl_2$ (Merck p.a.) followed by washing until Cl^- free and drying in static air at 383 K for 16 h. Each sample is exposed to gas treatments at different temperatures, indicated by [gas, z K, 1 h + y h]. This notation stands for a linear temperature increase in a certain gas flow during 1 h up to z K followed by an isothermal period at z K for y h.

[†] Interfacultair Reactor Instituut.
[‡] Schuit Institute of Catalysis.

S1089-5647(98)01401-1 CCC: $15.00
Published on Web 07/03/1998

All samples are calcined [air, 673 K, l h + 2 h] and kept in ambient air at room temperature to become saturated with water. Only the hydrated Co(4.0)NaY sample is divided into two parts, one of which is sulfided as prepared (referred to as wet Co(4.0)NaY). The other hydrated samples are subjected to an additional drying procedure [He, 673 K, l h + 2 h] and kept in a water free atmosphere. These samples are referred to as dry Co(2.4)NaY, Co(4.0)NaY, and Co(8.5)NaY. Except for the above calcination and He drying step, all subsequent treatments have been performed in situ in an EXAFS reactor.[13]

The hydrated and predried CoNaY samples are pressed in ambient air into self supporting wafers and mounted in the EXAFS cells. The thickness of these wafers is chosen such that the absorption μx is about 2.5 to give an optimal signal to noise ratio in the EXAFS spectra. To eliminate the water adsorbed during pressing the dry Co(2.4, 4.0, and 8.5)NaY samples are subjected to an additional drying step [He, 673 K, l h + 2 h] in the EXAFS cell.

Next, each CoNaY sample is stepwise sulfided in a 10 vol % H_2S/H_2 gas mixture, [H_2S, *z* K, l h + l h], at the following (*z* K) temperatures 300, 373, 473, 573, and 673 K. After each sulfiding step, the samples are cooled in H_2S/H_2 atmosphere to room temperature. Finally, the cell is flushed with helium and left at a pressure of 1.7 bar. Each EXAFS spectrum is measured at liquid N_2 temperature.

For the MES study two additional samples were prepared containing 2.0 and 8.0 wt % Co and doped with ^{57}Co, 66.6 Mbq. The Co(2.0)NaY sample is prepared in the same way as Co(4.5)NaY described in ref 1. A Co(8.0)NaY is prepared by adding an excess of Co^{2+} ions to the exchange solution. Then, the obtained sample is washed three times, spin dried and finally dried in static air at 383 K. The thus obtained Co(8.0)NaY is exchanged once more with a solution containing only the ^{57}Co and washed and dried as described above. After dehydration [He, 673 K, l h + l h] the samples are stepwise sulfided in the same sequence as the EXAFS samples.

For convenience sake, in the following paragraphs a fresh (i.e., non-sulfided) ion exchanged sample or an ion exchanged sample that is sulfided at *z* K will be indicated for example by wet Co(*x*)NaY(fresh) or dry Co(*x*)NaY(*z* K), respectively. (With wet and dry standing for the hydrated or dehydrated sample, respectively, and with *x* standing for *x* wt % Co.)

EXAFS Measurements and Data Analysis. The EXAFS spectra at the Co K-edge are measured at EXAFS station 8.1 at the SRS in Daresbury (U.K.). The storage ring was operated at 2.0 GeV, the ring current was in the range of 180−250 mA. The Si (220) monochromator was detuned to 70% intensity to remove higher harmonics in the X-ray beam.

Four scans are recorded after each gas treatment. The XDAP program version 2.0.3[14] is used for data manipulation and analyses. The EXAFS oscillations in *k*-space are obtained from the X-ray absorption spectra by subtracting a Victoreen curve followed by a cubic spline background removal.[15] The obtained chi-function is normalized by the height of the edge (jump). To analyze the spectra, phase shifts and backscattering amplitudes from reference compounds are used. For the Co−S reference, the coordination in CoS_2 is measured at station 8.1. CoS_2 has an octahedral coordination of cobalt by sulfur at a distance of 2.315 Å.[16] The structure of the CoS_2 sample (Johnson Matthey 99.9%) is checked by XRD (Cu K source). The Ni−Ni coordination in NiO obtained by Bouwens et al.[17] is used as a Co−Co reference. The use of a Ni absorber instead of a Co absorber is justified because the phases and backscattering amplitudes of neighboring elements such as Co and Ni hardly differ.[18] In the case of a Co−O and a Co−Si coordination, a theoretical reference is calculated with FEFF-code 3.11.[19] Vaarkamp et al.[20] stated that the FEFF code is the best one to use for calculating references.

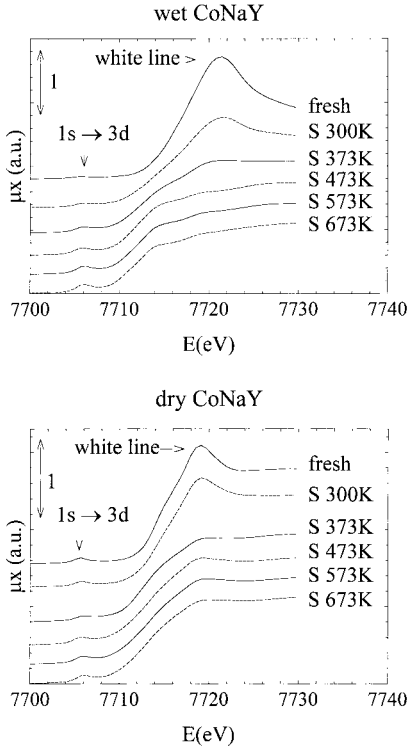

Figure 1. (a) XANES region of wet Co(4.0)NaY after successive sulfidation steps. (b) XANES region of dry Co(4.0)NaY after successive sulfidation steps.

All EXAFS results are produced by fitting in *r*-space until a satisfactory fit is obtained for k^1- and k^3-weighted spectra in *r*-space as well as *k*-space. The various FT ranges used are chosen between 2.68 and 12.58 $Å^{-1}$. The ranges for the *r*-fit are between 0.6 and 4.0 Å. Because we are studying the formation/growth of cobalt−sulfide particles in a wide range of sulfidation temperatures, distributions of different Co−sulfide phases will be present in certain samples. This can lead to difficulties to determine the different contributions due to fitting problems. Therefore, to prevent the fitting program to produce nonphysical data in these cases some parameters are kept fixed or constrained.

In the next paragraphs to indicate different peak positions in the presented FT-functions the notation of *x* Å (uncorr) (uncorr = uncorrected) is used, with *x* standing for the position at the *x*-axis as indicated in the figures. When (uncorr) is not added (i.e., *x* Å), the deduced corrected bond distances are given.

MES Measurements and Data Analysis. For more details on the executed MES neasurements, the used equipment, the data analysis, etc., the reader is referred to refs 1 and 11.

Results

XANES: Sulfidation of Wet and Dry Co(4.0)NaY. The Co K-edges (XANES-region) of wet and dry Co(4.0)NaY in the fresh and various sulfided states are given in Figure la and b, respectively. For both type of catalysts the edge shape is changing upon increasing the sulfidation temperature. Almost all XANES-regions show a preedge peak near 7706 eV. This is caused by the 1s → 3d transition which is more intense in tetrahedral than in octahedral coordination of the absorbing atom.[5,21,22] Wet Co(4.0)NaY(fresh) shows a very small (low

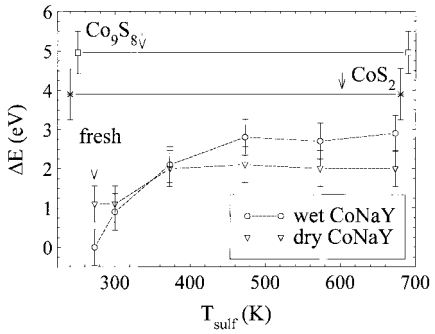

Figure 2. The chemical shifts of wet and dry Co(4.0)NaY after successive sulfidation steps, relative to the Co K-edge of wet Co(4.0)-NaY(fresh).

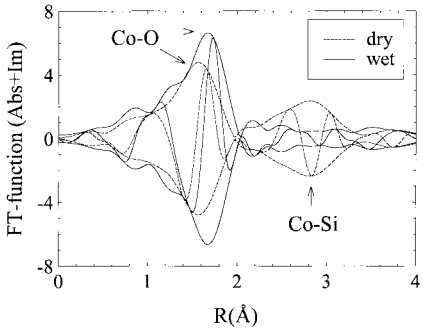

Figure 3. K^3-weighted FT functions (Abs + Im) of wet and dry Co-(4.0)NaY(fresh).

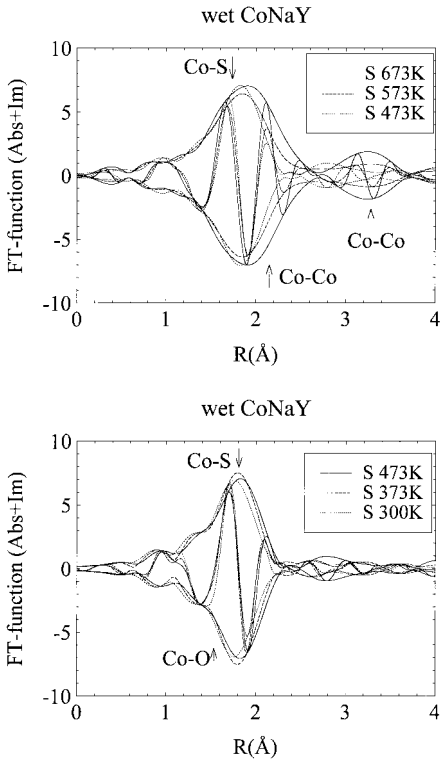

Figure 4. (a) K^3-weighted FT functions (Abs + Im) of wet Co(4.0)-NaY(300, 373, and 473 K). (b) K^3-weighted FT functions (Abs + Im) of wet Co(4.0)NaY(473, 573, and 673 K).

intensity) preedge peak, but its intensity is increased with increasing sulfidation temperature indicating that the coordination of Co is changing from an almost octahedral surrounding to one lower than six. Figure lb shows no distinct intensity changes in the preedge peak for dry CoNaY and indicates a coordination number lower than six in the first coordination shell. It follows from these XANES features that wet and dry Co(4.0)NaY(fresh) samples are different.

It is also shown in Figures la,b that both fresh Co(4.0)NaY samples exhibit a large white line. However, the white line area of wet Co(4.0)NaY(fresh) is larger than that of dry Co-(4.0)NaY(fresh). In both cases the white line area decreases with increasing sulfidation temperature. Upon room temperature sulfidation, this decrease is much larger for wet Co(4.0)NaY than for dry Co(4.0)NaY. After sulfidation at 473 K, the white line has disappeared for wet Co(4.0)NaY, whereas for dry Co-(4.0)NaY still after sulfidation at 673 K a very small "white line" exists.

In addition, it can be seen that the absorption edges shift to lower energies upon increasing sulfidation temperature, with the shift of dry CoNaY(673K) being smaller than that of wet CoNaY(673 K). Lytle and Greegor[23] described this so called "chemical" shift as follows. The edge position is determined not by valence alone, but also by bond distance and the way the scattering from neighboring atoms folds back down the edge. The chemical shifts relative to the position of the Co K-edge of wet Co(4.0)NaY(fresh) (7715 eV) are shown in Figure 2 (a positive shift means a shift of the Co K-edge to a lower energy). Drying of wet Co(4.0)NaY(fresh) causes a chemical shift of 1.1 eV. Besides, the shape of the Co K-edges of both fresh samples are different (see Figure l). These observations, together with the change of the preedge peak, clearly indicate that the valence of the Co atom and/or its first neighbor coordination changes when the starting material ion exchanged wet Co(4.0)NaY is carefully dried. In Figure 2 also the chemical shifts of two bulk reference compounds (CoS_2 and Co_9S_8) are included. Co in CoS_2 is octahedrally surrounded by sulfur, whereas Co_9S_8 contains tetrahedrally as well as octahedrally coordinated Co in a ratio 8:1. It is clear that the chemical shifts found for wet and especially for dry Co(4.0)-NaY(673K) remain lower than those of bulk CoS_2 and Co_9S_8.

From the above it can be concluded that the local Co environment is different for wet and dry Co(4.0)NaY in the fresh state. Both samples behave differently upon sulfidation resulting in different local Co environments after sulfidation at 673 K.

EXAFS: Sulfidation of Wet Co(4.0)NaY. In Figure 3 the FT spectra of wet and dry Co(4.0)NaY(fresh) are compared. For wet Co(4.0)NaY(fresh) only one single strong backscattering peak in the radial distribution function is observed, in contrast with dry Co(4.0)NaY(fresh) which shows two strong backscattering peaks. The imaginary part of the first main peak of the FT function of wet Co(4.0)NaY(fresh) indicates the presence of an oxygen surrounding (Co−O) in the first coordination shell. (Whether a contribution in the first main backscattering peak is mainly due to a Co−O or a Co−S coordination can be decided in a simple way as follows: In case of a Co−O coordination, the imaginary part peaks positive at the right side of the maximum of the absolute value, whereas Co−S peaks positive at the left.) The absence of well defined large contributions at longer distances show that Co is present in the form of small or disordered species.

The FT-functions obtained after stepwise sulfidation of wet Co(4.0)NaY are presented in Figure 4a (300−473 K) and b (473−673 K). The peak position and the imaginary part of the first main peak in the FT function has clearly changed. For wet Co(4.0)NaY(300 K), this points to a more sulfidic environment (Co−S), in stead of the oxidic environment (Co−O) found for wet Co(4.0)NaY(fresh) (compare Figures 3 and 4a). Upon increasing sulfidation temperature (573 K and 673 K) the first

TABLE 1: EXAFS Parameters of Wet Co(4.0)NaY after Successive Sulfidation Steps[a]

	Co−O$^{(1)}$				Co−S$^{(1)}$				Co−Co$^{(1)}$				Co−Co$^{(2)}$				Co−Co$^{(3)}$			
T_{sulf} (K)	N	R (Å)	$\Delta\sigma^2$ (Å^2 × 10^{-3})	ΔE_0 (eV)	N	R (Å)	$\Delta\sigma^2$ (Å^2 × 10^{-3})	ΔE_0 (eV)	N	R (Å)	$\Delta\sigma^2$ (Å^2 × 10^{-3})	ΔE_0 (eV)	N	R (Å)	$\Delta\sigma^2$ (Å^2 × 10^{-3})	ΔE_0 (eV)	N	R (Å)	$\Delta\sigma^2$ (Å^2 × 10^{-3})	ΔE_0 (eV)
fresh	5.7	2.07	4.6	1	*b*	*b*	*b*	*b*	*b*	*b*	*b*	*b*	*b*	*b*	*b*	*b*	*b*	*b*	*b*	*b*
300	5.9	2.08	6.1	−6	1.2	2.31	0.3	−14	*b*	*b*	*b*	*b*	*c*	*c*	*c*	*c*	*c*	*c*	*c*	*c*
373	2.5	2.05[d]	6.7	−6	3.4	2.26[d]	1.8	0	*b*	*b*	*b*	*b*	0.2	2.9	−6.6	3	0.2	3.4	−5.4	1
473	*b*	*b*	*b*	*b*	5.1	2.21[d]	6.0	10	*b*	*b*	*b*	*b*	1.3	3.0	7.3	−1.8	*c*	*c*	*c*	*c*
					1.5	2.34[d]	0.2	−9												
573	*b*	*b*	*b*	*b*	4.8	2.21	4.3	8	1.3	2.6	7.3	−15	2.8	3.1	29	−15	1.8	3.6	6.1	−16
					0.6	2.34	−4.8	−3												
673	*b*	*b*	*b*	*b*	6.1	2.22	4.9	3	3.5	2.5	12	−20	*b*	*b*	*b*	*b*	2.9	3.5	3.7	−11
					1.0	2.37	−3.6	−8												

[a] Co−X$^{(1)}$ = first Co-X contribution present (X = O, S, Si, Co), Co−X$^{(2)}$ = second, etc. Uncertainties first shell parameters: coordination number, $N \pm 20\%$; coordination distance, $R \pm 0.04$ Å, Debye-Waller factor, $\Delta\sigma^2$ (Å^2) ± 20%; inner potential correction, ΔE_0 (eV) ± 10%. Co_9S_8: Co(t)−S: $R = 2.13$ Å, $N = 1$, and $R = 2.23$ Å, $N = 3$. Co(o)−S: $R = 2.36$ Å, $N = 6$. Co(t)−Co(t): $R = 2.51$ Å, $N = 3$. Co(t)−Co(t): $R = 3.47$ Å, $N = 3$ and $R = 3.54$ Å, $N = 3$ (t and o denote a tetrahedral and an octahedral cobalt atom, respectively).[25] [b] Contribution not present. [c] Contribution could not be determined. [d] Kept fixed (as mentioned in the text) from the beginning of the fit optimizing procedure.

main backscattering peak is broadened due to the appearance of a second contribution under this peak (at the right side of the Co−S contribution, see indications in Figure 4b). This contribution is most probably due to the high Z-scatterer Co (Co−Co). Also, a contribution appears at a longer distance ($R \approx 3.2$ Å, uncorr) whose intensity increases with increasing sulfidation temperature. The position of this contribution in the EXAFS spectrum is comparable with the second Co−Co contribution in Co_9S_8. Even contributions beyond 4.0 Å (uncorr) are found, indicating the presence of a well defined Co−sulfide structure. It can be concluded that upon increasing sulfidation temperature the Co in wet Co(4.0)NaY is transforming from small/disordered species with Co−O contributions into a well defined cobalt−sulfide "bulk" structure resembling that of Co_9S_8.

The EXAFS parameters deduced for the various wet Co(4.0)-NaY fresh and sulfided states are given in Table 1. For Co-(4.0)NaY(fresh) a Co−O contribution is found with a coordination number of 5.7 at a distance of 2.07 Å (the correct combination of N and $\Delta\sigma^2$ is determined by k^1 and k^3 fitting[24]). This coordination number is also expected from the absence of the 1s → 3d transition in the XANES region (see Figure 1), which points to a coordination number of six in the first coordination shell.

After sulfidation at 300 K, a Co−O (at 2.08 Å) and a Co−S (at 2.31 Å) contribution are deduced. This combination points to the influence of the H_2S/H_2 gas mixture already at room temperature. In Figure 4a, between 2.5 and 3.0 Å (uncorr), other contributions which are very small, are also present, which could not be determined within the chosen parameter constrains. However, in line with wet Co(4.0)NaY(373 K), they could be due to very small Co−Co contributions. After the next sulfidation step (373 K), N_{Co-O} has decreased in favor of a coordination by S. From studying the FT function of wet Co-(4.0)NaY(373 K) phase corrected for either the Co−O or Co−S phase, decreasing Co−O and Co−S distances is deduced with respect to those found in wet Co(4.0)NaY(300 K). The phase corrected spectra show a Co−O and Co−S distance of 2.05 and 2.26 Å, respectively. Therefore, these distances are kept fixed during the fit optimization procedure. Besides, from analyzing the difference spectrum (the calculated Co−O$^{(1)}$ and Co−S$^{(1)}$ are subtracted from the overall EXAFS spectrum), the presence of two very small Co−Co contributions at 2.9 and 3.3 Å became apparent.

In the FT spectrum recorded after the final (673 K) sulfidation step, the main peak is fitted following a procedure similar to that used in the case of the impregnation type dry Co(4.0)/NaY-(673 K).[11] The averaging fitting procedure as applied by Bouwens et al.[17] did not result in a satisfactory fit. Only by limiting the FT range to 4.0−10.0 Å^{-1}, could the FT-spectrum of wet Co(4.0)NaY(673 K) be analyzed with one sulfur contribution at 2.22 Å (fixed) and one cobalt contribution at 2.55 Å (fixed) (the distances found for sulfided Co/C by Bouwens et al.[17]). When the FT range was increased (3.17−12.44 Å^{-1}), the sulfur contribution in the main peak had to be split into two contributions to obtain a satisfactory fit, while additionally it was necessary to keep some parameters under control (the distances and Debye−Waller factors). Two contributions, instead of one Co−S contributions, are assumed at distances around 2.21 and 2.34 Å, which are more or less the same as those present in the crystallographic structure of bulk Co_9S_8 (see note in Table 1 of ref 25). In comparison with the results obtained for Co(4.0)NaY(573 K) presented below, sulfidation at 673 K leads to an increase of both Co−S$^{(1)}$ and Co−Co coordination numbers (see Table 1). Furthermore, a Co−Co$^{(3)}$ contribution is found at a distance of 3.5 Å, which is also present in bulk Co_9S_8.[25] This Co−Co$^{(3)}$ contribution has become larger compared to CoNaY(573 K), and no other Co−Co contribution is needed to produce a good fit for the second peak in the FT function.

After sulfidation at 573 K, cobalt−sulfide particles have grown and became more structured in comparison with wet Co-(4.0)NaY(473 K). A Co−Co$^{(3)}$ contribution is deduced at a distance of 3.6 Å. In addition, a Co−Co$^{(2)}$ contribution at 3.1 Å is chosen in order to stay in line with the results found for Co(4.0)NaY(373 and 473 K). The deduced Co−Co$^{(2)}$ contribution could only be fitted with a very large Debye−Waller factor ($\Delta\sigma^2 = 0.029$) pointing to a rather disordered structure. Also the possibility to analyze this contribution by a Co−S contribution (also with a very large $\Delta\sigma^2$) indicates the difficulties in determining these small contributions.

After sulfidation at 473 K, the XANES region shows no Co−O interaction any more (see Figure la). Therefore, the main peak will consist of only a Co−S contributions or a combination of Co−S and Co−Co contributions. In the latter case, it was impossible to obtain a satisfactory fit. Only one Co−S contribution, N_{Co-S} of 6.2 at a distance of 2.26 Å, is determined. Although still not perfect, this fit could be improved by applying a similar procedure to that used before for Co(4.0)NaY(573 and 673 K). Two contributions instead of one Co−S contributions, are assumed at (fixed) distances of 2.21 and 2.34 Å. At 3.0 Å, a Co−Co contribution is found. The small contributions

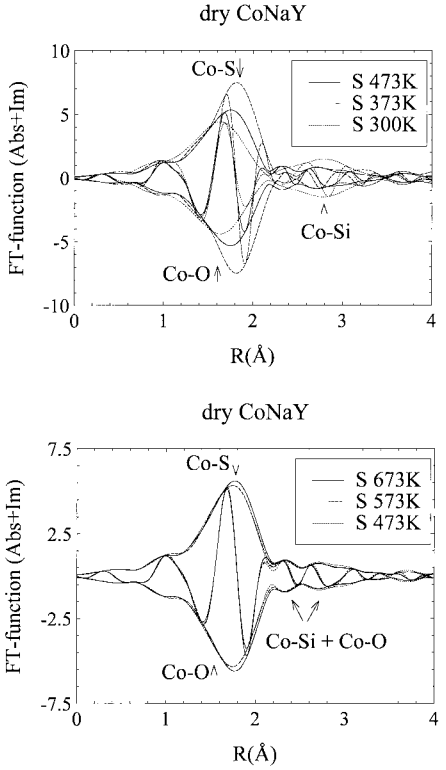

Figure 5. (a) K^3-weighted FT functions (Abs + Im) of dry Co(4.0)-NaY(300, 373, and 473 K). (b) K^3-weighted FT functions (Abs + Im) of dry Co(4.0)NaY(473, 573, and 673 K).

observed at longer distances could not be identified, probably due to their disordered structure. However, by comparison of wet Co(4.0)NaY(473 K) with wet Co(4.0)NaY(373 and 573 K), it can be concluded that these contributions are most probably arising from Co atoms at longer distances. Adding these contributions did not influence the fitting results of the main peak presented in Table 1.

Summarizing, it is shown that upon increasing sulfidation temperature the Co present in wet Co(4.0)NaY is transforming from small/disordered Co−O species into a well defined Co−sulfide "bulk" structure, probably comparable with Co_9S_8. The growth of these Co−sulfide particles takes place via the formation of various intermediate states.

EXAFS: Sulfidation of Dry Co(4.0)NaY. The FT function of dry Co(4.0)NaY(fresh) is compared with that of wet Co-(4.0)NaY(fresh) in Figure 3. Upon dehydration, the Co^{2+} ions in ion exchanged CoNaY occupy zeolite cation positions.[26−28] This effect is reflected in the presence of the second backscattering peak, which is mainly due to a Co−Si contribution.[27,28] Such a strong second backscattering peak was also observed by Dooryhee et al.[29,30] on a dehydrated ion exchanged NiNaY. In addition, dry Co(4.0)NaY(fresh) shows pronounced contributions at distances up till 5.5 Å (uncorr). The imaginary part of the first backscattering peak of dry Co(4.0)NaY(fresh) indicates an oxygen surrounding (Co−O). These results point to an increase of the Co−NaY lattice interaction upon drying.

The FT functions found after the successive sulfidation steps of dry ion exchanged Co(4.0)NaY are presented in Figure 5a (300−473 K) and b (473−673 K). As for dry Co(4.0)NaY-(fresh), the oxygen surrounding is also dominant for dry Co-(4.0)NaY(300 K). Therefore, it seems that at room temperature contact with H_2S/H_2 has much less influence on the dry Co-(4.0)NaY than it has on wet Co(4.0)NaY. This confirms the stronger bonding (fixation) of the Co atom to the zeolite lattice after drying. After sulfidation at 373 K, the peak position and the imaginary part of the first backscattering peak has changed indicating the presence of a Co−S contribution. At the same time, the strong second backscattering peak and longer distance contributions (R > 4.0 Å, uncorr) have disappeared. At higher sulfidation temperatures (473, 573, and 673 K) the FT functions remain more or less constant, pointing to similar local environments of the Co atom (Figure 5b).

Summarizing, it can be concluded that upon increasing sulfidation temperature the local environment of the Co atoms in dry Co(4.0)NaY is changing from a well defined/ordered structure (Co−NaY interaction) into the environment of a small/disordered Co−sulfide particle.

Due to interferences of different Co−O and Co−Si contributions in the first and second backscattering peak, the dry Co-(4.0)NaY(fresh) FT function was hard to fit. From XRD analysis[26] is known that depending on dehydration temperature the Co^{2+} ions will partly migrate to the hexagonal prisms (zeolite cation position I) and to other cation positions present in NaY. An attempt to fit these different Co−O contributions present in the zeolite did not succeed. A $Co-O^{(1)}$ contribution at 2.00 Å and a $Co-Si^{(1)}$ one at 3.2 Å are certainly present. However, both contributions did not cover the FT function of dry Co-(4.0)NaY(fresh) in Figure 3. Their coordination numbers are strongly influenced by adding Co−O contributions at about 3.0 and 3.5 Å (zeolite cation positions I′ and I, respectively[26]). Adding these contributions did not result in a large improvement of the fitting results and large uncertainties still remained. Therefore, only the $Co-O^{(1)}$ (the correct combination of N and $\Delta\sigma^2$ is determined by k^1 and k^3 fitting[24]) and $Co-Si^{(1)}$ (the deduced coordination distance) contributions are presented in Table 2. But it has to be kept in mind that most probably additional Co−O and/or Co−Si contributions are present in dry Co(4.0)NaY(fresh).

The first main backscattering peak of dry Co(4.0)NaY(300K) contains more than only one Co−O contribution around 2.00 Å. A minimum of two contributions is necessary to obtain a satisfactory fit of the first main peak. The small shift to a higher distance and a slight change of the imaginary part of this first main peak (compare Figures 3 and 5a) indicate the presence of a small Co−S contribution. By adding a $Co-S^{(1)}$ at 2.31 Å it is possible to cover the right side of this FT peak. Due to interference between the contributions present the exact $N_{Co-O(1)}$, $R_{Co-O(1)}$ and $N_{Co-S(1)}$, $R_{Co-S(1)}$ are difficult to determine. It also turns out that the Co−Si contribution (at 3.3 Å) in the second backscattering peak is decreased, although this contribution is depending on adding a Co−O contribution at 3.0 Å (zeolite cation site I′, see also relevant text about dry Co(4.0)NaY-(fresh)). Therefore, the results presented for dry Co(4.0)NaY-(300 K) in Table 2 have to be considered as indications of a trend and not as exact numerical results.

It is clear that the changes in the FT function upon sulfidation (373−673 K) are caused by removing the Co^{2+} ions from the different zeolite cation positions, which is reflected in the large decrease of the second backscattering (Co−Si) peak. To fit the spectra of dry CoNaY(373−673 K), the following procedure is applied: the $Co-S^{(1)}$ is determined by k^1 and k^3 fitting to find the correct combination of N and $\Delta\sigma^2$ [24] (N is around 5.2). Then it turns out that addition of a small contribution at the left side of the main peak (short distance) is necessary. From the white lines (Figure 1b), chemical shifts (Figure 2) and Mössbauer emission spectroscopy results (the presence of a small high-spin 2+ contribution[1]), a Co−O contribution seems the best choice. By the addition of a small contribution of

TABLE 2: EXAFS Parameters of Dry Co(4.0)NaY after Successive Sulfidation Steps[a]

	Co−O(1)				Co−S(1)				Co−Si(1)				Co−O(2)			
T_{sulf} (K)	N	R (Å)	$\Delta\sigma^2$ (Å^2 × 10^{-3})	ΔE_0 (eV)	N	R (Å)	$\Delta\sigma^2$ (Å^2 × 10^{-3})	ΔE_0 (eV)	N	R (Å)	$\Delta\sigma^2$ (Å^2 × 10^{-3})	ΔE_0 (eV)	N	R (Å)	$\Delta\sigma^2$ (Å^2 × 10^{-3})	ΔE_0 (eV)
fresh	3.5	2.00	3.7	1	*b*	*b*	*b*	*b*	3−2	3.2	*c*	*c*	*c*	*c*	*c*	*c*
300	4.3	2.00	7.0	2	0.9	2.31	−0.3	−3	2−3	3.3	*c*	*c*	*c*	*c*	*c*	*c*
373	0.1	1.89	−7.8	17	5.3	2.25	2.3	5	0.6	3.0	−1.3	18	0.8	3.4	−5.8	−11
473	0.2	1.89	−0.7	17	5.4	2.21	6.2	9	0.5	2.8	−0.3	5	2.4	3.4	1.4	6
573	0.2	1.91	−0.7	17	5.3	2.22	6.2	8	0.6	2.8	1.1	5	2.8	3.4	4.6	6
673	0.3	1.89	1.3	17	5.2	2.23	5.7	7	0.7	2.8	1.6	6	2.7	3.4	4.7	6

[a] Co−X(1) = first Co-X contribution present (X = O, S, Si, Co), Co−X(2) = second, etc. Uncertainties first shell parameters: coordination number, N ± 20%; coordination distance, R ± 0.04 Å, Debye−Waller factor, $\Delta\sigma^2$ (Å^2) ± 20%, inner potential correction, ΔE_o (eV) ± 10%. [b] Contribution not present. [c] Contribution could not be determined.

oxygen at a distance of about 1.9 Å (the Co−S contribution is kept constant), the fitting of the main peak indeed improved.

The contributions at longer distances are determined by subtraction of the calculated Co−S(1) and Co−O(1) contributions from the overall EXAFS spectrum and by fitting the difference spectrum. A Co−Si(1) contribution is found. Upon increasing sulfidation temperature (373−673 K) the N and R of this Co−Si(1) contribution stay more or less constant. An additional contribution most likely originates from a Co−O(2) contribution at a distance of 3.4 Å with a coordination number increasing to about 2.7. The fact that this contribution could be exchanged by a Co−Si(2) contribution indicates that the various contributions at longer distances can not be determined unambiguously. The presence of a Co−Si(1) and Co−O(2) at a longer distance is in accordance with the results obtained by Mössbauer emission spectroscopy (see reference 1), which demonstrate the presence of a Co−zeolite lattice interaction even after sulfidation at 673 K. Attempts to fit any Co−Co contribution in the obtained difference spectrum were not successful, which gives an indication that no significant clustering of Co atoms has taken place. The thus deduced results are presented in Table 2, which shows that after sulfidation at 473, 573, and 673 K the Co−S(1) coordination and distance are almost constant.

Summarizing, it is shown that upon increasing sulfidation temperature Co present in dry Co(4.0)NaY is transformed into Co−sulfide particles by removing the Co^{2+} ions from the NaY cation positions and changing their environment into a sulfidic one. This results in the formation of very small or disordered Co−sulfide particles, whereas for wet Co(4.0)NaY formation of "bulk" Co_9S_8 particles was observed.

EXAFS and MES: Comparison of Dry Co(x)NaY ($x \approx$ 2, 4, or 8 wt %). The influence of the Co loading on the Co−sulfide dispersion is only studied for dry Co(x)NaY being the catalyst system that enables the formation of the highly dispersed Co−sulfide species aimed for. Therefore, additional samples containing about 2 and 8 wt % Co are prepared and studied with EXAFS and MES.

After sulfidation at 300 K a remarkable difference is found between the EXAFS results of Co(2.4)NaY on the one hand and those of Co(4.0)NaY and Co(8.5)NaY on the other. In the main peak of the radial distribution function of Co(2.4)NaY a Co−S contribution dominates, whereas for Co(4.0 and 8.5)-NaY a Co−O contribution is the dominating one.

In Figure 6 the FT functions of Co(x)NaY (x = 2.4, 4.0, or 8.5) after sulfidation at 673 K are presented. The intensity of the main peak decreases upon increasing Co loading indicating a slight decrease in coordination number. The imaginary part of all three main peaks point to a sulfidic environment. At uncorrected distances longer than 2 Å the 4.0 and 8.5 wt % CoNaY are almost identical, whereas Co(2.4)NaY shows a somewhat different envelope. As shown in Table 3, Co(4.0)-NaY and Co(8.5)NaY could indeed be fitted in the same way (Co−Si(1) and Co−O(1) contribution). However, in the case of the Co(2.4)NaY it is impossible to determine the contributions above 2 Å (uncorr). Possible contributions are from O, S, Si, or Co. Therefore, in this case only the fit parameters of the main peak are presented in Table 3.

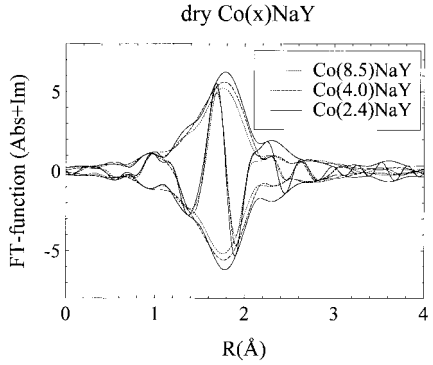

Figure 6. K^3-weighted FT functions (Abs + Im) of dry Co(x)NaY-(673 K), with x = 2.4, 4.0, and 8.5 wt %.

TABLE 3: EXAFS Parameters of Dry Co(x)NaY (x = 2.4, 4.0, and 8.5 wt %) after Sulfidation at 673 K[a]

	Co−O(1)		Co−S(1)		Co−Si(1)		Co−O(2)	
x (wt %)	N	R (Å)	N	R (Å)	N	R (Å)	N	R (Å)
2.4	0.5	1.90	5.6	2.24	*b*	*b*	*b*	*b*
4.0	0.3	1.91	5.2	2.23	0.7	2.8	2.7	3.4
8.5	0.3	1.89	4.7	2.22	0.8	2.8	2.7	3.4

[a] Uncertainties first shell parameters: coordination number, N ± 20%, coordination distance, R ± 0.04 Å. [b] Contribution could not be determined.

The MES results obtained after sulfidation at 673 K are presented in Figure 7 and Table 4. The main quadrupole doublet is assigned to Co−sulfide particles (the contribution with an IS ≈ 0.23 mm/s). All samples show a large QS value (QS ≈ 0.70 mm/s) of the Co−sulfide doublet after sulfidation at 673 K. The other component of the MES spectrum represents a group of different Co species (a distribution in IS and QS). The IS and QS values presented in Table 4 for the distribution IS + QS contribution have to be considered as mean values. These results clearly show that with increasing Co loading the quadrupole splitting of the main Co−sulfide doublet remains more or less constant. However, the mean QS value for the second contribution (distribution of IS + QS) is increasing with increasing Co loading. This "distribution" probably originates from a combination of species with a large QS value (due to a Co−O interaction) and a small QS value (due to a Co−S interaction) (For more details on this subject, see ref 1). In that case it follows from the increasing mean QS value with

TABLE 4: MES Parameters of Dry Co(*x*)NaY (*x* = 2.0, 4.5, and 8.0 wt %) after Sulfidation at 673 K[a]

	Co−sulfide				distribution IS + QS				
x (wt %)	IS (mm/s)	QS (mm/s)	Γ (mm/s)	*A* (%)	IS (mm/s)	QS (mm/s)	Γ_1 (mm/s)	Γ_2 (mm/s)	*A* (%)
2.0	0.23	0.66	0.66	54	0.63	0.91	1.70	0.57	46
4.5	0.20	0.63	0.78	69	0.82	1.39	1.21	0.54	31
8.0	0.27	0.73	0.72	56	0.81	1.64	1.34	0.76	44

[a] Isomer shift: IS ± 0.03 mm/s. Quadrupole splitting: QS ± 0.03 mm/s. Line width: $\Gamma_{1,2}$ ± 0.05 mm/s. Spectral contribution: *A* ± 5%.

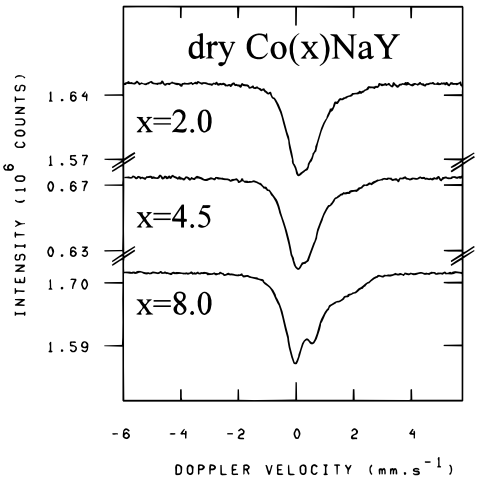

Figure 7. The MES spectra of dry Co(*x*)NaY(673 K), with *x* = 2.0, 4.5, and 8.0 wt %.

increasing cobalt loading that the amount of Co interacting with the zeolite lattice slightly increases with increasing cobalt loading.

Summarizing, the above results show that no Co−Co clustering takes place with increasing cobalt loading. The only observed difference is a slight increase in the Co−NaY lattice interaction.

Discussion

On the basis of QS value variations observed in the MES spectra, Crajé et al.[7] have proposed a structural model for the Co−sulfide species formed during sulfidation of carbon and alumina supported Co and CoMo catalysts. In this model, the Co−sulfide species is a very small particle characterized by its *size* and *ordering*. The *particle size* indicates the number of Co atoms that is associated with a Co−sulfide particle, while the Co−sulfide is said to be more *ordered* the better its coordination parameters agree with those of Co_9S_8. Furthermore, a decreasing QS value reflects the growth and/or increasing ordering of highly dispersed Co−sulfide to particles showing IS and QS values characteristic for Co_9S_8.

In refs 1 and 11, a rapidly decreasing QS value of the Co−sulfide doublet (IS = 0.19−0.29 mm/s) of wet CoNaY to a value of QS = 0.22 mm/s (T_{sulf} = 473 K) is reported, whereas for dry CoNaY a rather large value of QS = 0.63 mm/s is observed. (It is important to note that, in wet CoNaY(473 and 573 K), 48% and 16% of the Co was present as CoS_{1+x} (IS = 0.35−0.39 mm/s)[1,11], respectively, and that dry CoNaY(473−673K) contained a distribution in high-spin $2+^1$ (30% probably due to a Co−NaY lattice interaction).)

In the following, the present EXAFS and MES results together with the previously published MES results[1,11] will be discussed in terms of the above mentioned structural model.

Differences between Wet and Dry Co(4.0)NaY(fresh). The XANES (Figures la and b and 2) and EXAFS (Figure 3) results show a number of differences between wet (hydrated) and dry (dehydrated) Co(4.0)NaY(fresh). Firstly, there is the difference in Co−O coordination number in the first main contribution. Secondly, a large second backscattering peak appears upon dehydration. Thirdly, the intensity of both preedge peaks and white lines in the XANES region differs. Fourthly, a chemical shift of 1.1 eV is observed after dehydration.

The Co−O coordination number of 5.7 deduced for wet Co(4.0)NaY(fresh) is comparable with the one found by Morrison et al.,[31] who found by EXAFS that Co^{2+} ions in wet (hydrated) NaY are surrounded by six H_2O molecules. Such a coordination number is also suggested by Dooryhee et al.[29,30] for hydrated Ni^{2+} ions inside NaY. These last authors additionally suggested the presence of a Ni−Si contribution with a N_{Ni-Si} of 4 at a distance of 3.3 Å. Such an additional Co−Si contribution at 3.3 Å could not be fitted satisfactory in the FT function of wet Co(4.0)NaY(fresh).

Upon dehydration the Co(4.0)NaY(fresh) sample, striking changes are observed. The Co−O coordination decreases from 5.7 to 3.5 (see Table 2), which is in agreement with the increasing intensity of the 1s → 3d transition in the XANES region. The cobalt−zeolite lattice interaction increases due to migration of the Co^{2+} ions to the zeolite cation positions, reflected by the appearance of the large second backscattering peak (see Table 2, Co−Si at 3.2 Å). Such a contribution around *R* = 3.2 Å is also found by Moller and Bein[28] (for dehydrated CoNaY) and Morrison et al.,[27] who also found a Co−O contribution of 3.3 at 1.97 Å for dehydrated CoNaA. In addition, Gallezot and Imelik[26] concluded from their XRD study that migration of Co^{2+} ions into several zeolite cation positions takes place upon dehydration. They found Co−O that the coordination number of 3.5 points to an almost tetrahedral surrounding. This observation suggests that the Co^{2+} ions are mainly positioned in the II, II′, or I′ cation sites of the NaY zeolite. This tetrahedral coordination of dehydrated CoNaY was found earlier by Egerton et al.[32] (magnetic studies) and Bonardet et al.[33] Both suggested that the Co^{2+} ions are mainly positioned in the six-membered ring of the sodalite cages (probably site II′). Egerton et al.[32] showed that only after full dehydration the Co^{2+} ions would be positioned in the hexagonal prisms (site I) and would be octahedrally coordinated. The above mentioned literature results confirm our interpretation of the dry Co(4.0)-NaY(fresh) EXAFS spectrum, although not all spectral contributions could be conclusively deduced.

The shift of the absorption edge upon drying Co(4.0)NaY with 1.1 eV implies a change of the nearest neighbors coordination around the Co^{2+} ions. This change is confirmed by the Co−O coordination numbers deduced from the FT functions. However, these differences between wet and dry Co(4.0)NaY-(fresh) observed by EXAFS and XANES are not reflected in the MES spectra shown earlier.[1] Wet and dry CoNaY(fresh) showed identical MES spectra. Only a difference is found in the normalized resonant absorption area (RAA) which has increased upon drying. Such an increase indicates a better bonding (fixing) of the Co^{2+} ions to the NaY lattice.

In contrast herewith, MES analysis clearly showed that drying

of Co(4.0)NaY has a large influence on its sulfidation behavior and so did EXAFS and XANES.

Sulfidation of Wet Co(4.0)NaY. The chemical shift between wet Co(4.0)NaY(fresh) and wet Co(4.0)NaY(300K) or wet Co(4.0)NaY(673K) has a value of 0.9 or 2.9 eV, respectively (see Figure 2). Therefore, the local environment of Co is changing with increasing sulfidation temperature. EXAFS shows after sulfidation at 300 K the presence of a Co−O and a Co−S contribution together with small contributions at longer distances. This points to the presence of Co^{2+} ions at easily accessible positions (i.e., the supercages) and to a weak bonding between these Co^{2+} ions and their surrounding (H_2O molecules) inside the NaY.

In the fresh state, an average of 8.7 Co atoms are present in one unit cell containing 8 supercages, 8 sodalite cages, and 16 hexagonal prisms. Therefore, an average of 1.1 Co atoms is present inside one supercage. After sulfidation at 373 K, clearly the presence of a Co−Co interaction is found at 2.9 and 3.4 Å. These $Co-Co^{(2)}$ and $Co-Co^{(3)}$ contributions increase with increasing sulfidation temperature, clearly indicating migration of cobalt atoms to each other. After sulfidation at 573 and 673 K, two Co−Co contributions appeared at distances also present in crystalline Co_9S_8 (see note at Table l) viz. $Co-Co^{(1)}$ at 2.5 Å and $Co-Co^{(3)}$ at 3.5 Å. At the same time (673 K), the $Co-Co^{(2)}$ contribution at 3.0 Å, which is not present in crystalline Co_9S_8, disappeared. From these findings it can be concluded that after sulfidation at 673 K well ordered Co_9S_8 type particles are formed. However, their crystallinity is lower than that of bulk Co_9S_8[25] and lower than the crystallinity of the Co−sulfide particles formed in impregnation type dry sulfided Co(4.0)/NaY-(673 K).[11] In the case of this impregnation type sample, additionally the $Co-Co^{(3)}$ contribution had to be split into two in order to produce a totally covering fit, most probably due to the better crystallinity of the Co−sulfide species present.

The formation of well ordered Co−sulfide particles is confirmed by the MES results,[1] showing a 100% spectral contribution with a QS value of 0.22 mm/s which is ascribed to Co_9S_8 species. The presence of the $Co-Co^{(2)}$ contribution in the EXAFS spectrum after sulfidation at 473 and 573 K suggests that the formation of Co_9S_8 takes place via intermediate phases which is corroborated by the MES results. After sulfidation at 473 K, the presence of a spectral contribution (48%) assigned to CoS_{1+x} (see refs 1 and 11) is found while the other part of the Co is present in a Co_9S_8 structure, which spectral contribution increases upon increasing sulfidation temperature. As the interatomic distances in CoS_{1+x} (R_{CO-S} = 2.34 Å and R_{Co-Co} = 2.59 Å,[34]) are almost identical to the distances in Co_9S_8 (R_{Co-S} = 2.23 Å and R_{Co-Co} = 2.5l Å) these two structures will not be distinguishable in the EXAFS spectrum.

Because the location of the Co−sulfide particles (at the inner or outer NaY surface) cannot be deduced from the MES and EXAFS results, HREM is applied (experimental details are the same as described for an impregnation type dry sulfided Co/NaY[11]). After sulfidation at 473, 573, and 673 K, large cobalt−sulfide particles are found at the outer zeolite surface. For instance, wet Co(4.0)NaY(673 K) contained particles in the range of 15−50 nm at the outer zeolite surface. In Figure 8 a typical example of a wet Co(4.0)NaY(673 K) electron micrograph is shown.

The formation of the relatively large Co_9S_8 particles outside the NaY structure explains the relatively low initial thiophene HDS activity measured after sulfidation at 473, 573, and 673 K.

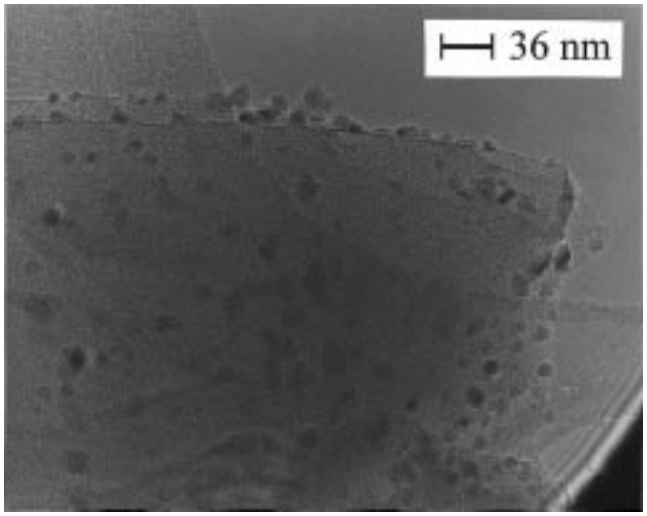

Figure 8. HREM picture of wet Co(4.0)NaY(673 K).

Hence, the results deduced from the EXAFS and HREM measurements clearly show that sulfidation of ion exchanged Co(4.0)NaY in the presence of physisorbed water leads to the formation of large and well ordered Co_9S_8 species at the outer NaY surface and are in agreement with the MES and thiophene HDS results presented earlier.[1]

Sulfidation of Dry Co(4.0)NaY. The chemical shift between dry Co(4.0)NaY(fresh) and Co(4.0)NaY(673 K) of 0.9 eV is much smaller than the shift of 2.9 eV in the case of wet Co-(4.0)NaY (see Figure 2). This difference indicates that the local environment of Co in dry Co(4.0)NaY and wet Co(4.0)NaY is changing differently. In the sulfidation temperature range 373−673 K the chemical shift (see Figure 2) of dry Co(4.0)NaY remains constant. Additionally, EXAFS shows that after sulfidation at 300 K no Co−O is removed in favor of a Co−S contribution and that the second main contribution $Co-Si^{(1)}$ is still present. This points to a strong bonding between the Co^{2+} ions and NaY lattice. Most probably the Co atoms in the zeolite are present at positions unreachable for H_2S such as the cation sites in the sodalite cages and hexagonal prisms. However, after sulfidation at 373 K almost all Co−O has disappeared and is replaced by a Co−S contribution. The Co^{2+} ions present on the different NaY cation sites in the fresh state have been (partly) removed from their positions upon increasing sulfidation temperature. In contrast with wet Co(4.0)NaY, no Co−Co contribution is found not even at the highest sulfidation temperature. This shows that the Co−sulfide species are probably very small entities existing of only one Co atom with a neighboring shell of sulfur. The observation of the higher shells ($Co-Si^{(1)}$ and $Co-O^{(2)}$) indicate the presence of a Co−NaY interaction. However, the detailed "structure" of these contributions can not be deduced, most probably due to the presence of a large variety of Co species (a Co−sulfide contribution and a distribution in IS + QS) as observed in the MES spectrum of Co(4.5)NaY (see Figure 7).

The most important EXAFS result is the absence of any Co−Co contribution. This strongly indicates that we are dealing here with very small Co−sulfide entities inside the NaY supercages. The presence of such a small Co−sulfide entity is also reflected in the QS value (0.63 mm/s) of the MES spectrum (see Figure 7), which is much higher than the value found for wet CoNaY(673 K) (QS = 0.22 mm/s). HREM analysis of dry Co(4.0)NaY shows that after sulfidation at various (300−673 K) temperatures no Co−sulfide particles are present at the outer zeolite surface (see the electron micrograph of dry Co-

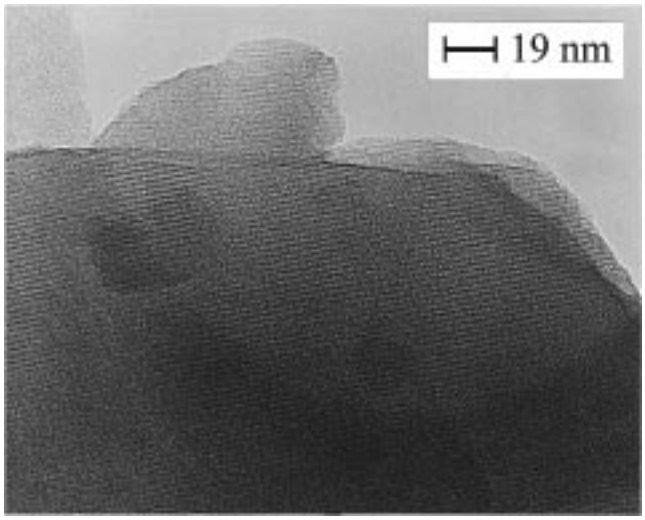

Figure 9. HREM picture of dry Co(4.0)NaY(673 K).

(4.0)NaY(673 K) in Figure 9). This in combination with EDX analysis proves the presence of Co and S inside the NaY lattice. Therefore, in clear contrast with wet Co(4.0)NaY(673 K) Co−sulfide in dry Co(4.0)NaY(673 K) is essentially present as very small particles inside the NaY supercages. This explains the high initial thiophene HDS activity after sulfidation at 473, 573, and 673 K.[1]

Hence, EXAFS and HREM results clearly show that sulfidation of ion exchanged Co(4.0)NaY in the absence of physisorbed water leads to the formation of small Co−sulfide species and this is in agreement with the earlier MES and thiophene HDS results.[1]

Influence of Cobalt Loading on the Sulfidation of Dry Co(*x*)NaY (*x* ≈ 2, 4, or 8 wt %). After sulfidation at 673 K, a subtle decrease in Co−S coordination number with increasing Co loading is found by EXAFS analysis (see Table 3, $N_{Co-S(1)}$). The MES measurements presented in Figure 7 show a slight increase of the high-spin 2+ contribution indicating a slight increase of the Co−zeolite lattice interaction (Co−oxygen) upon increasing Co loading, reflected in the increasing QS value of the distribution in IS + QS contribution (see Table 4). As explained in the section results, this contribution is not well defined and probably originates from a combination of species with a large QS value (due to Co−O interaction) and a small QS value (due to a Co−S interaction). As was to be expected, these subtle differences between the three MES spectra could not be reproduced by EXAFS analysis (see Table 3 and Figure 6).

Because the QS value of the Co−sulfide doublet in the MES spectra after sulfidation at 673 K is more or less constant with different Co loadings (2, 4, and 8 wt % Co corresponding with 0.5, 1.1, and 2.3 Co atoms per supercage, respectively) and a Co−Co interaction is not found in the EXAFS spectra, it can be concluded that the Co loading does not affect the Co−sulfide dispersion.

Conclusions

The EXAFS results presented in this study are clearly a complement to the results obtained earlier[1] by MES and thiophene HDS activity measurements.

The sulfidation of ion exchanged Co(4.0)NaY in the presence of physisorbed water results in the formation of relatively large and well ordered Co_9S_8 species which are positioned at the outer NaY surface and have a relatively low initial thiophene HDS activity. This formation takes place via an intermediate phase (CoS_{1+x}).

Sulfidation of ion exchanged Co(4.0)NaY in the absence of physisorbed water results in the formation of very small highly dispersed Co−sulfide entities inside the NaY supercages with a very high initial thiophene HDS activity.

The Co loading in dry Co(*x*)NaY (*x* = 2, 4, or 8 wt %) does not affect the high dispersion of the Co−sulfide species inside the supercages.

Acknowledgment. The authors thank Dr. L.A. Medici for lending his EXAFS equipment and his kind assistance during the EXAFS measurements, Dr. M. Oversluisen of the SRS, Daresbury Laboratory, for his help during the EXAFS measurements, and Dr. H. Zandbergen of the National Centre for High Resolution Electron Microscopy of the Delft University of Technology for performing and discussing the HREM measurements. This project has been financially supported by the Dutch organization scientific research, NWO, and by SON-STW, Project: 349-3356. This work has been performed under the auspices of NIOK, the Netherlands Institute of Catalysis Research, Lab Report 98-3-01.

References and Notes

(1) de Bont, P. W.; Vissenberg, M. J.; Boellaard, E.; van Santen, R. A.; de Beer, V. H. J.; van der Kraan, A. M. *Bull. Soc. Chim. Belg.* **1995**,-*104*, 205.

(2) Minderhoud, J. K.; van Veen, J. A. R. *Fuel Process. Technol.* **1993**, *35*, 87.

(3) Crajé, M. W. J.; de Beer, V. H. J.; van der Kraan, A. M. *Bull. Soc. Chim. Belg.* **1991**, *100*, 953.

(4) Crajé, M. W. J. Ph.D. Thesis, Interfacultair Reactor Instituut, Delft University of Technology, Delft, 1992 (ISBN 90-73861-08-X).

(5) Crajé, M. W. J.; Louwers, S. P. A.; de Beer, V. H. J.; Prins, R.; van der Kraan, A. M. *J. Phys. Chem.* **1992**, *96*, 5445.

(6) Crajé, M. W. J.; de Beer, V. H. J.; van Veen, J. A. R.; van der Kraan, A. M. *J. Catal.* **1993**, *143*, 601.

(7) Crajé, M. W. J.; de Beer, V. H. J.; van Veen, J. A. R.; van der Kraan, A. M. *Hydrotreating Technology for Pollution Control. Catalysts, Catalysis and Processes;* Occelli, M. L., Chianelli, R., Eds.; Marcel Dekker, Inc.: New York, 1996; p 95.

(8) Ward, J. W. *Stud. Surf. Sci. Catal.* **1983**, *16*, 587.

(9) Ward, J. W. *Fuel Process. Technol.* **1993**, *35*, 55.

(10) Leglise, J.; Janin, A.; Lavalley, J. C.; Cornet, D. *J. Catal.* **1988**, *114*, 388.

(11) de Bont, P. W.; Vissenberg, M. J.; Boellaard, E.; de Beer, V. H. J.; van Veen, J. A. R.; van Santen, R. A.; van der Kraan, A. M. *J. Phys. Chem. B* **1997**, *101*, 3072.

(12) Topsøe, H.; Clausen, B. S.; Candia, R.; Wivel, C., Mørup, S. *J. Catal.* **1981**, *68*, 433.

(13) Kampers, F. W. H.; Maas, T. M. J.; van Grondelle, J.; Brinkgreve, P.; Koningsberger, D. C. *Rev. Sci. Instrum.* **1989**, *60*, 2635.

(14) Vaarkamp, M.; Linders, J. C.; Koningsberger, D. C. To be published.

(15) Cook, J. W.; Sayers, D. E. *J. Appl. Phys* **1981**, *52*, 5024.

(16) Elliott, N. *J. Chem. Phys.* **1960**, *33*, 903.

(17) Bouwens, S. M. A. M.; van Veen, J. A. R.; Koningsberger, D. C.; de Beer, V. H. J.; Prins, R. *J. Phys. Chem.* **1991**, *95*, 123.

(18) Teo, B. K.; Lee, P. A. *J. Am. Chem. Soc.* **1979**, *101*, 2815.

(19) Mustre de Leon, J.; Rehr, J. J.; Zabinsky, S. I.; Albers, R. C. *Phys. Rev. B* **1991**, *44* (9), 4146.

(20) Vaarkamp, M.; Dring, I.; Oldman, R. J.; Stern, E. A.; Koningsberger, D. C. *Phys. Rev. B* **1994**, *50* (11), 7872.

(21) Bouwens, S. M. A. M.; Koningsberger, D. C.; de Beer, V. H. J.; Prins, R. *Catal. Lett.* **1988**, *1*, 55.

(22) Nieman, W.; Clausen, B. S.; Topsøe, H. *Catal. Lett.* **1990**, *4*, 355.

(23) Lytle, F. W.; Greegor, R. B. *Phys. Rev. B* **1988**, *37* (4), 1550.

(24) Kampers, F. W. H. Ph.D. Thesis, Schuit Institute of Catalysis, Eindhoven University of Technology, Eindhoven, 1988.

(25) Rajamani, V.; Prewit, C. T. *Can. Mineral.* **1975**, *13*, 75.

(26) Gallezot, P.; Imelik, B. *J. Chim. Phys.* **1974**, 155.

(27) Morrison, T. I.; Iton, L. E.; Shenoy, G. K.; Stucky, G. D.; Suib, S. L.; Reis, A. H. *J. Chem. Phys.* **1980**, *73*, 4705.

(28) Moller, K.; Bein, T. *Zeolites: Facts, Figures, Future*; Jacobs, P. A., van Santen, R. A., Eds.; Elsevier Science Publishers B. V.: Amsterdam, 1989; p 985.

(29) Dooryhee, E.; Greaves, G. N.; Steel, A. T.; Townsend, R. P.; Carr, S. W.; Thomas, J. M.; Catlow, C. R. A. *Faraday Discuss. Chem. Soc.* **1990**, *89*, 119.

(30) Dooryhee, E.; Catlow, C. R. A.; Couves, J. W.; Maddox, P. J.; Thomas, J. M.; Greaves, G. N.; Steel, A. T.; Townsend, R. P. *J. Phys. Chem.* **1991**, *95*, 4514.

(31) Morrison, T. I.; Reis, A. H.; Gebert, E.; Iton, L. E.; Stucky, G. D.; Suib, S. L. *J. Chem. Phys.* **1980**, *72*, 6276.

(32) Egerton, T. A.; Hagan, A.; Stone, E. S.; Vickerman, J. C. *J. Chem. Soc. Faraday Trans. I* **1972**, *68*, 723.

(33) Bonardet, J. L.; Gédéon, A.; Fraissard, J. *Stud. Surf. Sci. Catal.* **1995**, *94*, 139.

(34) Kuznetsov, V. G.; Sokolova, M. A.; Palkina, K. K.; Popova, Z. V. *Inorg. Mater. USSR* **1965**, *1*, 617.